CHEMISTRY
A EUROPEAN JOURNAL

DOI: 10.1002/chem.201000155

Counterion Effects on the Columnar Mesophases of Triphenylene-Substituted [18]Crown-6 Ethers: Is Flatter Better?

Martin Kaller,[a] Christopher Deck,[a] Annette Meister,[b] Gerd Hause,[c] Angelika Baro,[a] and Sabine Laschat*[a]

Dedicated to Professor Franz Effenberger on the occasion of his 80th birthday

Abstract: The twisted lateral tetraalkyloxy *ortho*-terphenyl units in dibenzo[18]crown-6 ethers **1a–f** were readily converted into the flat tetraalkyloxytriphenylene systems **2a–f** by oxidative cyclization with $FeCl_3$ in nitromethane. Reactions of the latter with potassium salts gave complexes KX·**2**, which displayed mesomorphic properties. The aromatization increased both the clearing and melting points; the mesophase stabilities, however, were mainly influenced by the respective anions upon complexation with various potassium salts. In contrast, the alkyl chain lengths played only a secondary role. Among the potassium complexes of triphenylene-substituted crown ethers KX·**2**, only those with the soft anions I^- and SCN^- displayed mesophases with expanded phase temperature ranges of 93 °C and 132 °C (for KX·**2e**), respectively, as compared to the corresponding *o*-terphenyl-substituted crown ether complexes KI·**1e** ($\Delta T = 51$ °C) and KSCN·**1e** (plastic crystal phase). Anions such as Br^-, Cl^-, and F^- decreased the mesophase stability, and PF_6^- led to complete loss of the mesomorphic properties of KPF_6·**2** although not for KPF_6·**1**. For crown ether complexes KX·**2** (X = F, Cl, Br, I, BF_4, and SCN), columnar rectangular mesophases of different symmetries (*c*2*mm*, *p*2*mg*, and *p*2*gg*) were detected. In contrast to findings for the twisted *o*-terphenyl crown ether complexes KX·**1**, the complexation of the flat triphenylene crown ethers **2** with KX resulted in the formation of organogels. Characterization of the organogel of KI·**2e** in CH_2Cl_2 revealed a network of fibers.

Keywords: anions · crown compounds · ion pairs · liquid crystals · mesophases · salt effects

Introduction

Columnar liquid crystals have been extensively investigated over the last decades because their structural and physical properties, such as one-dimensional (1D) charge transport and self-healing of defects, make them promising candidates for various applications, for example, organic light-emitting diodes, organic field-effect transistors, organic photovoltaic cells, gas sensors, high-resolution laser printers, and photocopying machines.[1] The attachment of crown ethers as substituents to mesogenic building blocks gives access to novel hybrid materials. Based on the pioneering observations by Percec and Ungar that complexation of crown ethers and azacrowns with metal salts leads to a significant stabilization of the mesophase,[2] many groups have entered the field and have developed, for example, conducting wires,[3] organic gelators,[3b,e,4] helical fibers that assemble at gel/graphite interfaces,[5] amphiphilic metallomesogens with high charge-carrier mobilities for high-performance organic field-effect transistors,[6] and membranes containing ion-selective transport channels.[7] However, with regard to structure–property relationships and the comparison of structurally related mesogens, the influence of metal ion complexation on the mesomorphic properties is less clear cut.[8–11]

Recently, we reported on dibenzo[18]crown-6 derivatives **1** with two lateral *ortho*-terphenyl units and their complexes MX·**1** ($M = K^+$, NH_4^+).[12] It turned out that the anion X has

[a] Dipl.-Chem. M. Kaller, Dipl.-Chem. C. Deck, Dr. A. Baro, Prof. Dr. S. Laschat
Institut für Organische Chemie der Universität Stuttgart
Pfaffenwaldring 55, 70569 Stuttgart (Germany)
Fax: (+49) 711-685-64285
E-mail: sabine.laschat@oc.uni-stuttgart.de

[b] Dr. A. Meister
Martin-Luther-Universität Halle-Wittenberg
HALOmem–Biophysical Chemistry of Membranes
Kurt-Mothes-Str. 3, 06120 Halle (Saale) (Germany)

[c] Dr. G. Hause
Martin-Luther-Universität Halle-Wittenberg, Biozentrum
Weinbergweg 23, 06120 Halle (Saale) (Germany)

Supporting information for this article is available on the WWW under http://dx.doi.org/10.1002/chem.201000155.

a much stronger effect on their properties than the alkyl chain length. The anion not only caused a stabilization (soft anions such as iodide and bridging anions such as hexafluorophosphate) or destabilization (hard anions such as fluoride, chloride, and tetrafluoroborate) of the mesophase as compared to neat crown derivatives **1**, but also influenced the mesophase type. Whereas the soft thiocyanate anion induced the formation of an ordered plastic crystal phase in KSCN·**1**, anions such as Hal^-, PF_6^-, and BF_4^- led to the formation of columnar mesophases.[12] Previous work by Müllen on graphene-type columnar liquid crystals revealed that the temperature ranges of the columnar mesophases of propeller-shaped hexaphenylbenzenes could be significantly increased by converting them to the corresponding hexa-*peri*-hexabenzocoronenes (HBC) with an extended flat aromatic system.[13,14] This stabilizing effect of the HBC unit was attributed to increased π-π interactions. In the light of these observations, we were interested to ascertain whether a related cycloaromatization of the *ortho*-terphenyl units in **1** to the corresponding triphenylene-substituted crown ethers **2** (Scheme 1) would lead to improved mesophase temperature ranges. Furthermore, we have focused on the study of the mesophase properties of potassium complexes KX·**2** with particular emphasis on the influence of the counterion. It was of interest to assess whether a certain anion could overrule or enhance the influence of the extended aromatic core. The results are reported below.

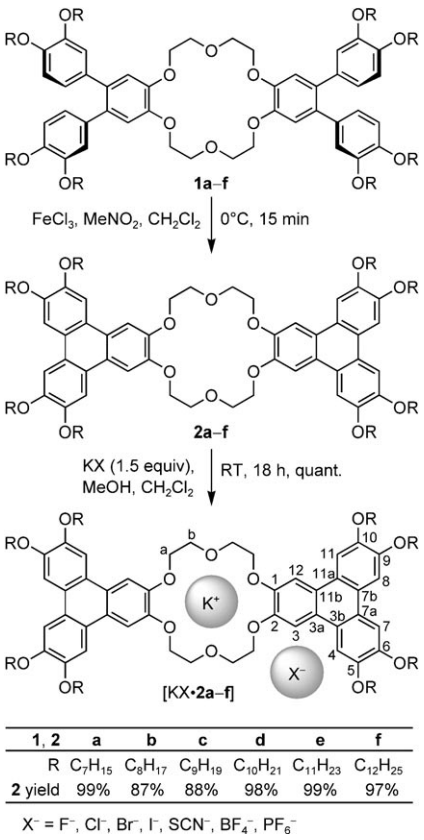

1, 2	a	b	c	d	e	f
R	C_7H_{15}	C_8H_{17}	C_9H_{19}	$C_{10}H_{21}$	$C_{11}H_{23}$	$C_{12}H_{25}$
2 yield	99%	87%	88%	98%	99%	97%

$X^- = F^-, Cl^-, Br^-, I^-, SCN^-, BF_4^-, PF_6^-$

Scheme 1. Synthesis of triphenylene-substituted crown ethers **2** and their complexes.

Results and Discussion

Synthesis and MALDI-TOF mass spectrometry of triphenylene-substituted crown ethers 2: The known crown ethers **1a–f** were prepared as described previously.[12] Several methods for cyclization of the *o*-terphenyl-substituted derivatives **1** were investigated. First, a system of VOF_3 as oxidant and $BF_3{\cdot}OEt_2$ as a Lewis acid was used, which has been successfully applied to the synthesis of triphenylene-substituted [15]crown-5 ethers.[8] However, in the case of **1b**,**d**, this procedure led to decomposition instead of cyclization, even within a reaction time of just 5 min. Replacement of $BF_3{\cdot}OEt_2$ by $B(OMe)_3$ gave the desired products **2b** and **2d**, respectively, but due to incomplete reaction, mixtures of educt and product (**1b**/**2b** and **1d**/**2d**) were obtained, which could not be separated by either recrystallization or column chromatography. Ma and Pei[15] reported the oxidative cyclization of *o*-terphenyl to triphenylene structures in almost quantitative yields by using $FeCl_3$ in nitromethane as a mild oxidant. By applying this method, the *o*-terphenyl substituents in **1a–f** could be conveniently transformed into triphenylene moieties (Scheme 1). For this cyclization reaction, an excess (15 equiv) of $FeCl_3$ in nitromethane was used. In order to prevent acid-catalyzed ether cleavage, the HCl evolved had to be removed by passing a vigorous stream of dry nitrogen through the mixture during the reaction. In this manner, crown ethers **2a–f** were accessible in good to quantitative yields (88–99%) in analytically pure form.[16]

Complexes KX·**2a–f** were prepared following a modification of the procedure reported by Pedersen.[12,17–19] A solution of the respective crown ether **2** (1 equiv) in CH_2Cl_2 was added to a solution of the appropriate potassium salt (1.5 equiv) in MeOH, and the resulting slurry was vigorously stirred overnight. After evaporation of the solvents, the residue was taken up in boiling CH_2Cl_2 and the solution was filtered. Concentration of the filtrate and drying of the residue under high vacuum afforded the respective target complex in quantitative yield. For KX·**2c** (KX = KF, KCl, KPF_6), KBr·**2e**, and KX·**2f** (KX = KCl, KBF_4, KPF_6), a 1:1 ratio of salt:crown could be verified by elemental analyses, while for the other salts complexation was deduced from the MALDI-TOF mass spectra,[12,20] as exemplified for neat crown ether **2e** and its KBr complex (Figure 1).

In the spectrum of neat **2e**, the molecular ion $[M]^+$ signal at $m/z = 2023.1$ was detected as the most intense peak, together with two small peaks at $m/z = 2046.1$ and 2062.2 due to the $[M+Na]^+$ and $[M+K]^+$ adducts (Figure 1a). The latter two peaks originated from traces of sodium salts in the potassium-free matrix and a potassium impurity in the sodium. Additionally, fragmentation of **2e** was observed under the conditions of the MALDI experiments. Up to three side chains were cleaved, giving rise to fragment ions $[M-C_{11}H_{23}]^+$, $[M-2C_{11}H_{23}]^+$, and $[M-3C_{11}H_{23}]^+$ at $m/z =$ 1867.8, 1712.5, and 1557.2, respectively. After complexation, a completely different picture emerged. The most intense peak in the spectrum of complexed **2e** was that of the $[M+K]^+$ adduct at $m/z = 2062.2$ (Figure 1b). Sodium–potas-

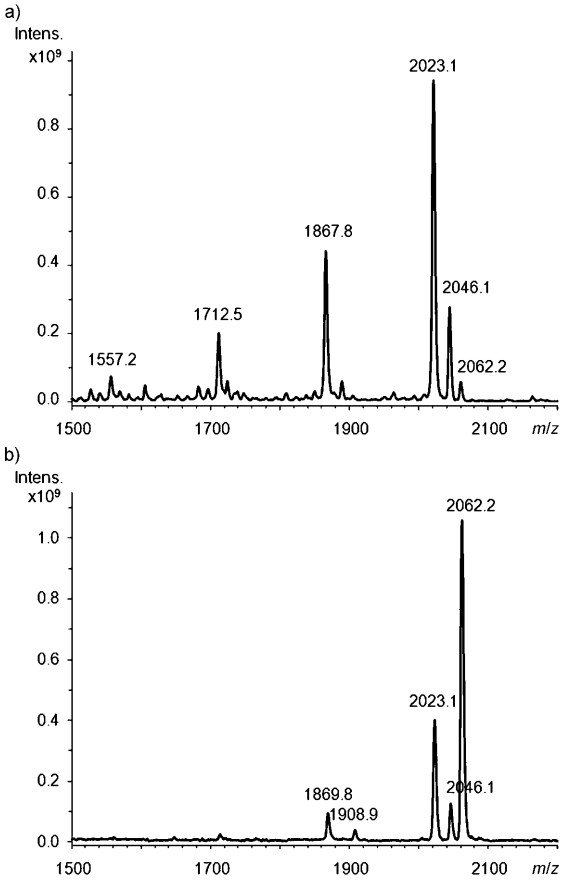

Figure 1. MALDI-TOF spectra of a) neat crown ether **2e**; b) complex KBr·**2e**.

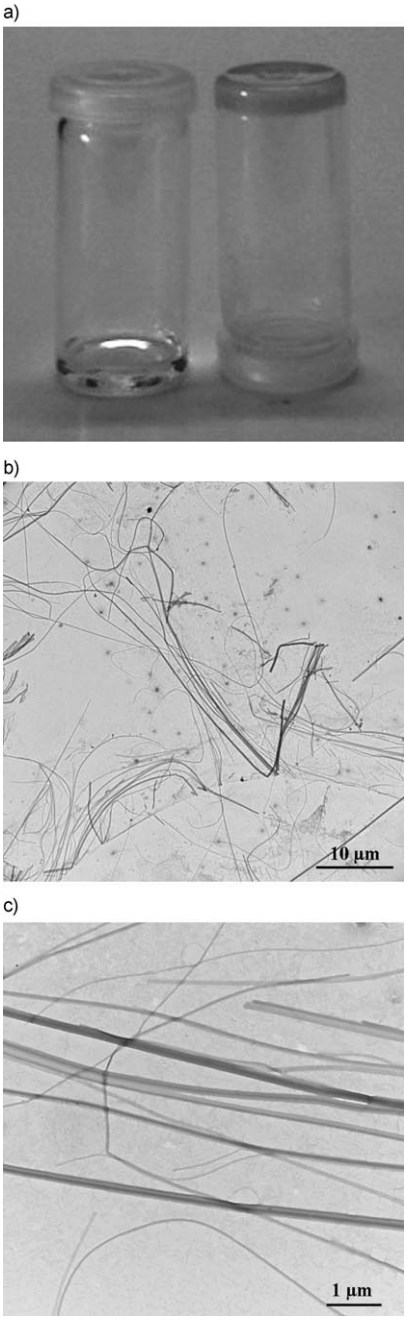

Figure 2. a) The left vial contains pure CH_2Cl_2, the right one the gel of KI·**2e** (ca. 11.4 mmol L^{-1}; 25.0 g L^{-1}) in CH_2Cl_2; b) and c) TEM images of the organic gelling agent KI·**2e** (0.01 mmol L^{-1}) at different magnifications. Fibers of different thicknesses form an entangled network.

sium exchange with the matrix and loss of potassium under the experimental conditions were responsible for low-intensity signals due to $[M+Na]^+$ at $m/z=2046.1$ and $[M]^+$ at $m/z=2023.1$. Surprisingly, the complex KBr·**2e** showed little tendency to undergo fragmentation and only one side chain was cleaved under MALDI conditions, yielding a potassium-complexed fragment ion $[M+K-C_{11}H_{23}]^+$ at $m/z=1908.9$ and an uncomplexed fragment ion $[M-C_{11}H_{23}]^+$ at $m/z=$ 1869.8. All of the complexes KX·**2** showed similar MALDI spectra, with the most intense signal being that due to $[M+K]^+$. This result was taken as evidence for stabilization of the system resulting from potassium cation uptake by the crown ether unit.

NMR spectroscopic analysis and gelling properties: In order to confirm the 1:1 crown:salt ratio and to gain insight into the structure of the complexes in solution, ^1H and ^{13}C NMR spectra were examined in detail.

Unlike the neat crown ether derivatives **2**, all of the complexes KX·**2** formed gels within a few minutes after dissolution in any of a multitude of organic solvents, including $CHCl_3$, CH_2Cl_2, MeOH, DMSO, MeCN, C_6H_6, and $C_2H_2Cl_4$ (Figure 2a). Transmission electron microscopy (TEM) showed that the organic gelling agent KI·**2e** self-assembles into fibers and ultimately forms an entangled network, which probably causes gelation of the liquid (Figure 2b,c). The network structure formed by the low molecular weight organogelator is held together solely by noncovalent forces, including hydrogen bonding, π stacking, and solvophobic effects. In recent years, there has been rapidly growing interest in low molecular weight gelling agents due to the potential applications of gels and their remarkable properties with respect to self-assembly phenomena.[21]

The time prior to gelation was long enough to record ^{1}H NMR spectra at room temperature, but was too short to acquire ^{13}C NMR spectra with good signal-to-noise ratios. Therefore, ^{13}C NMR spectra were recorded only for the series KX·**2e** at 355 K in $C_2D_2Cl_4$. For KPF_6·**2**, ^{1}H NMR spectra were also recorded at 355 K in $C_2D_2Cl_4$ because aggregation led to very broad signals at room temperature.

Comparing the ^{1}H NMR spectra of **2e** and KX·**2e** (Figure 3), striking differences could be noted with respect

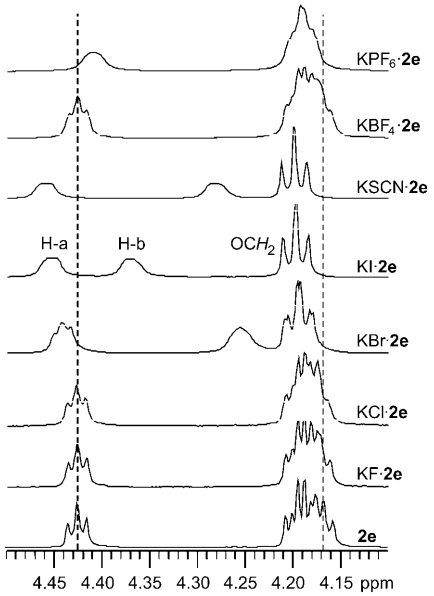

Figure 3. ^{1}H NMR spectra (500 MHz, $C_2D_2Cl_4$) of crown ether **2e** and its complexes KX·**2e**. For comparison, all spectra were measured at 355 K.

to the anions. In the ^{1}H NMR spectrum of neat **2e**, the H-a signal (for numbering, see Scheme 1) appears as a multiplet centered at $\delta = 4.43$ ppm. The H-b signal is overlapped by that of the OCH_2 groups of the alkyl side chains and appears as a multiplet at $\delta = 4.16$–4.21 ppm. After complexation, the H-a and H-b signals were variously shifted depending on the nature of the counterion. Slight downfield shifts together with line broadening were observed for KF·**2e** and KCl·**2e** with hard anions. The signals of H-a and H-b in complex KBr·**2e** were shifted downfield to $\delta = 4.44$ and 4.26 ppm, respectively. These effects were more pronounced for KI·**2e** and KSCN·**2e** with soft iodide and bridging thiocyanate, for which downfield shifts of $\Delta\delta = 0.02$–0.03 ppm (for H-a) and $\Delta\delta = 0.07$–0.16 ppm (for H-b) were observed. The complexation also affected the OCH_2 resonances, yielding pseudotriplets (**2e** complexed with KBr, KI, or KSCN).

From this downfield shift tendency, a 1:1 complexation of triphenylene-substituted crown ethers **2** was assumed, in analogy to observations on crown ether derivatives **1**[12] and literature findings concerning related [18]crown-6 complexes.[7,22–26] However, complexes KBF_4·**2e** and KPF_6·**2e** gave puzzling results. The H-b signals were slightly shifted downfield within the multiplets at $\delta = 4.16$–4.21 ppm, whereas for the H-a signals an upfield shift to $\delta = 4.41$ ppm was found for KPF_6·**2e**. Lockhart et al. proposed that an upfield shift of *all* crown ether signals can be taken as evidence for the presence of 2:1 complexes.[23] However, in the cases of KBF_4·**2e** and KPF_6·**2e** just the signals of the crown ether H-a protons were shifted upfield, while the H-b signals of the crown ether fragment showed downfield shifts. Presumably, this behavior may be caused by higher aggregates, for example, two connected tight ion pairs, rather than 2:1 complexation. The differential scanning calorimetry (DSC) data discussed below support this assumption.

Based on literature results,[23] upfield shifts of the signals of the relevant C atoms C-1, C-3, and C-a,b (for numbering, see Scheme 1) in the ^{13}C NMR spectra of complexes KX·**2** can be attributed to the presence of ion pairs. In the absence of ion pairing (hard anions F^-, Cl^-, or BF_4^-) only minor shifts were detected, whereas with soft anions (such as I^-), which are in close contact with the cation, and with strongly pairing anions (SCN^-, PF_6^-) large shifts up to $\Delta\delta \approx 2.4$ ppm were seen (see Figure S2 in the Supporting Information).

Mesomorphic properties of crown ethers 2 and their complexes: The mesomorphic properties of crown ethers **2a–f** and complexes KX·**2a–f** were studied by differential scanning calorimetry (DSC) (the detailed results are summarized in Tables S1–S8 in the Supporting Information), polarizing optical microscopy (POM), and wide-angle and small-angle X-ray scattering (WAXS, SAXS).

In the case of the neat crown ether derivatives **2a–f**, liquid-crystalline properties were only observed for **2c–f** with side-chain lengths C_9 to C_{12} (Figure 4a), and for these the mesophase temperature ranges were narrow (2–14 °C).

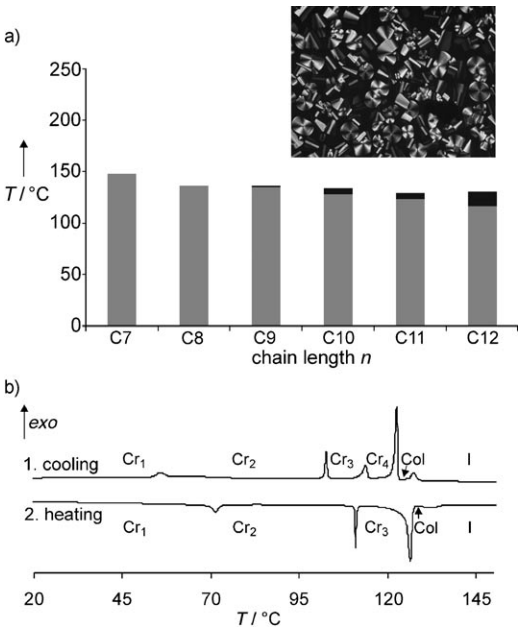

Figure 4. a) Mesophase stabilities of neat crown ether derivatives **2a–f** (Key: grey = Cr; black = Col) and texture micrograph of **2e** between crossed polarizers at 142 °C upon cooling from the isotropic phase (cooling rate 10 °C min^{-1}, magnification ×200); b) DSC curve of **2e** (heating/cooling rate 5 °C min^{-1}). Cr = crystal, Col = columnar, I = isotropic liquid.

Crown ether **2c** showed an isotropic-to-mesophase transition at 136 °C and crystallization at 135 °C upon first cooling. Upon second heating, isotropic melting at 139 °C was observed, demonstrating the monotropic behavior. Neat crown ethers **2d–f**, however, displayed enantiotropic mesophases, as exemplified for **2e**. Its DSC curve revealed an isotropic-to-mesophase transition at 129 °C, a crystallization at 123 °C, and three crystal-to-crystal transitions at 115, 103, and 58 °C upon first cooling (Figure 4b). Two crystal-to-crystal transitions at 70 and 111 °C, a melting transition at 125 °C, and a clearing point at 129 °C were found upon second heating. Under the microscope, compound **2e** was seen to form spherulithic textures typical of columnar mesophases (Figure 4a, inset). The phase type was assigned by X-ray diffraction analysis (see below).

The liquid-crystalline properties of the corresponding potassium halide complexes KHal·**2** upon first cooling and the typical textures observed are illustrated in Figure 5a–h. The KF complexes of **2a–c** were found to be non-mesomorphic and only crystal-to-crystal transitions were observed. For complexes KF·**2d–f**, enantiotropic mesophases were detected between 126 and 133 °C with small mesophase temperature ranges of 2–11 °C. The KF complexes of **2d–f** were seen to display spherulithic or broken fan-shaped textures under the microscope upon cooling, which are typical of columnar structures. The characteristic texture is exemplified by that of KF·**2e** (Figure 5e).

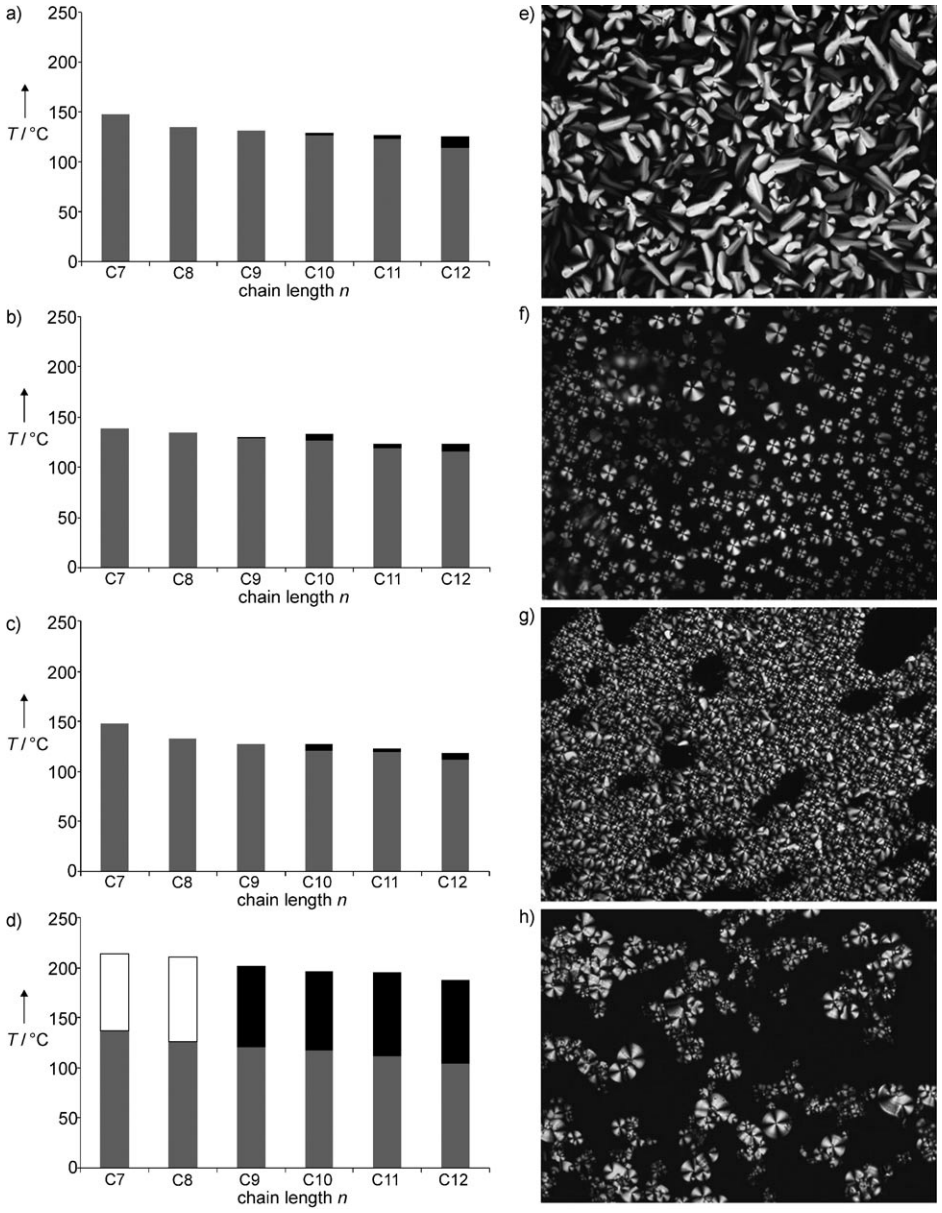

Figure 5. Mesophase stabilities upon first cooling (left, a–d) of halide complexes and typical textures (right, e–h) as seen between crossed polarizers upon cooling from the isotropic liquid (magnification ×200). a) KF·**2**; b) KCl·**2**; c) KBr·**2**; d) KI·**2** (Key: grey = Cr; black = Col; white = plastic); e) KF·**2e** at 129 °C (cooling rate 10 °C min^{-1}); f) KCl·**2e** at 132 °C (cooling rate 10 °C min^{-1}); g) KBr·**2f** at 118 °C (cooling rate 5 °C min^{-1}); h) KI·**2e** at 180 °C (cooling rate 10 °C min^{-1}).

A minimum chain length of C_9 was necessary in the series of complexes KCl·**2** for the formation of mesophases between 124 and 133 °C. The observed phases were monotropic in the case of KCl·**2c** and enantiotropic for KCl·**2d–f**, extending over a temperature range of 1–8 °C. Thus, complexation with KCl leads to an even stronger destabilization of the mesophases than that seen with KF. Spherulithic textures were observed by polarizing optical microscopy, indicating the presence of a columnar mesophase, as illustrated for complex KCl·**2e** (Figure 5f). The complexes with KBr gave some puzzling results. The complexes KBr·**2d–f** formed mesophases with very small temperature ranges (3–6 °C), while KBr·**2a–c** with C_7 to C_9 side-chain lengths were non-mesomorphic. For KBr·**2d** the mesophase was enantiotropic, whereas KBr·**2e**,**f** displayed only monotropic phases upon cooling, as illustrated by DSC of KBr·**2e** (Figure 6).

The DSC curve revealed crystal-to-crystal transitions at about 70 and 111 °C and isotropic melting at 121 °C upon second heating. Upon first cooling, however, an isotropic-to-

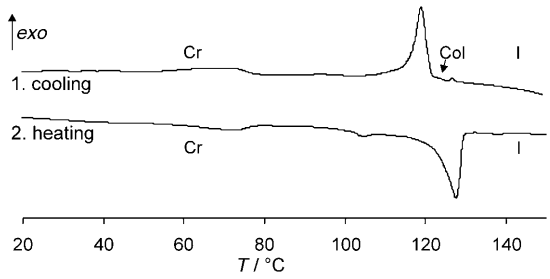

Figure 6. DSC curves of complex KBr·**2e**.

mesophase transition at 123 °C and crystallization at 120 °C were detected. Under the microscope, KBr·**2f** displayed a spherulithic texture typical of all complexes of the type KBr·**2** (Figure 5g).

In contrast, complexation of **2a–f** with KI led to a significant stabilization of the columnar mesophases. The whole series KI·**2** displayed enantiotropic (meso)phases. In the case of KI·**2a**,**b** plastic crystalline phases were found, whereas complexes KI·**2c–f** displayed columnar phases between 111 and 201 °C with large mesophase temperature ranges of 79–83 °C (Figure 5d). Melting and clearing points decreased with increasing side-chain length. Upon cooling from the isotropic liquid, spherulithic textures were observed, as, for example, for KI·**2e**, which confirmed the presence of a columnar phase (Figure 5h).

The liquid-crystalline properties of complexes KBF_4·**2** and KSCN·**2** upon the first cooling cycle are depicted in Figure 7a,c. Complexes KBF_4·**2** displayed enantiotropic mesophases for all side-chain lengths (Figure 7a). The DSC curve of KBF_4·**2e** (Figure 8) resembled that of neat **2e**. The complexation of **2e** with potassium tetrafluoroborate induced only minor changes in the phase behavior, with the exception of the clearing points, which were shifted to higher temperatures. Whereas a transition of the mesophase to the isotropic liquid was observed in the second DSC heating cycle (see Figure 8), upon cooling the clearing point was invisible and could only be detected by POM.

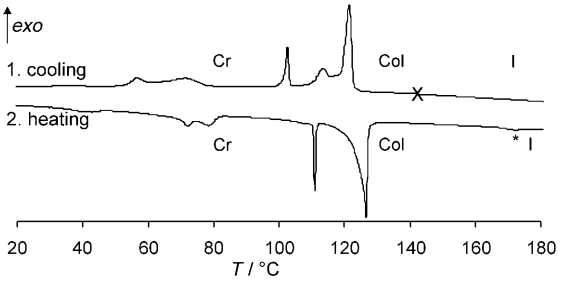

Figure 8. DSC curves of KBF_4·**2e**. * Clearing point observed in DSC; × clearing point observed using polarizing optical microscopy.

Strong supercooling caused a decrease of the mesophase temperature ranges to 11–40 °C as compared with those in the heating cycles (35–52 °C). The strong stabilization might be attributed to the weak pairing properties of the BF_4^- anion. Similar observations were made by Coco et al. for $KClO_4$ crown ether complexes.[6a] The typical texture of KBF_4·**2e**, with broken focal-conic fans characteristic of columnar mesophases, is shown in Figure 7b.

KSCN complexes of **2** were found to be thermally stable and displayed enantiotropic (meso)phases for all side-chain lengths. While KSCN·**2a** formed an ordered plastic phase (Figure 7c), the remaining complexes displayed columnar rectangular phases between 81 and 253 °C, extending over a broad temperature range of 133–172 °C. The columnar order of the mesophases was confirmed by the observation of extended spherulithic domains under the microscope upon cooling from the isotropic liquid (Figure 7d).

In contrast, all complexes KPF_6·**2** displayed isotropic melting with high melting points (233–266 °C) accompanied by decomposition. Presumably, the anion PF_6^- introduced such a high degree of order that mesomorphic properties were completely lost.

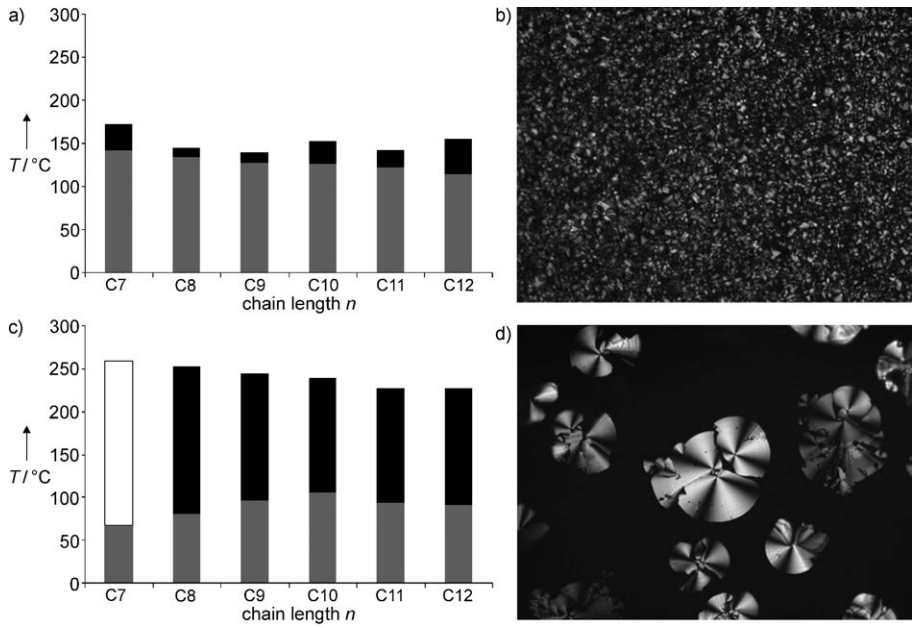

Figure 7. Mesophase stabilities upon first cooling of complexes a) KBF_4·**2**; c) KSCN·**2** (Key: grey = Cr; black = Col; white = plastic). Textures as seen between crossed polarizers upon cooling from the isotropic liquid (magnification ×200) of b) KBF_4·**2e** at 120 °C (cooling rate 10 °C min^{-1}); d) KSCN·**2e** at 243 °C (cooling rate 5 °C min^{-1}).

X-ray diffraction: In order to gain more insight into the nature of the mesophases of **2** and KX·**2**, temperature-dependent powder X-ray diffractograms were recorded (Table 1).

At room temperature, the samples showed intense sharp reflections at all angular positions, as befits crystalline phases. In the case of mesogenic derivatives, sharp reflections were only observed at small angles, whereas in the wide-angle region a broad scattering halo was detected, thus demonstrating the liquid-crystalline nature. The high number of reflections observed at small angles is indicative of columnar rectangular phases. Col_r phases of three different plane groups were found for crown ethers **2**.

Derivatives **2e**, **2f**, KF·**2d**, KF·**2e**, KCl·**2d**, KCl·**2e**, KBr·**2d**, and KBr·**2e** showed up to six characteristic reflections in the small-angle region, which were indexed as (20), (11), (31), (02), (22), and (60), respectively (Table 1, Figure 9a). However, (31) could also be (40) and (22) could also be (51), because both reflections have the same angular positions. The broad halo in the wide-angle regime origi-

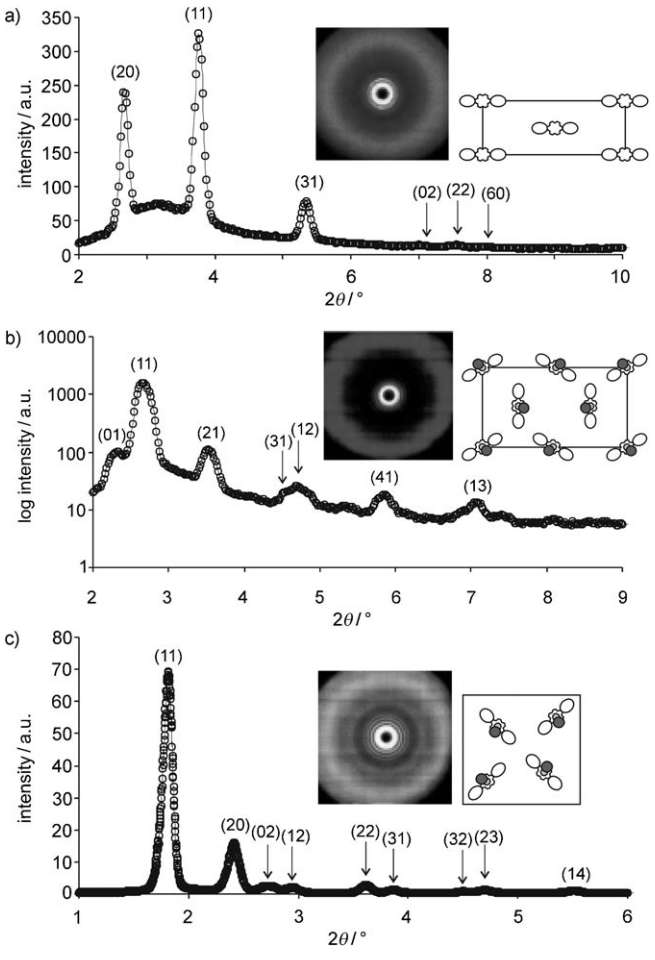

Figure 9. Small-angle scattering (SAXS) profiles of the liquid-crystalline phases of a) neat crown ether **2e** at 125 °C; b) complex KI·**2e** at 150 °C; and c) complex KSCN·**2e** at 140 °C (only the most intense reflections are shown). Insets: X-ray diffraction patterns (wide-angle scattering, WAXS) and schematic illustrations of the structural model for the unit cells: a) *c2mm* for **2e**; b) *p2mg* for KI·**2e**; c) *p2gg* for KSCN·**2e**.

Table 1. Summary of X-ray diffraction data collected for **2** and KX·**2**.

Compound	Mesophase	Lattice spacing/ Å	*d* spacing/ Å obsd (calcd)	Miller indices	ρ	$Z^{[a]}$
2e	Col_r at 125 °C *c2mm*	*a* = 66.1 *b* = 25.1	33.1 (33.1)	(20)	1.0	2.3
			23.5 (23.5)	(11)		
			16.5 (16.5)	(31),(40)		
			12.5 (12.5)	(02)		
			11.7 (11.7)	(22),(51)		
			11.0 (11.0)	(60)		
			4.6 (halo)	–		
2f	Col_r at 120 °C *c2mm*	*a* = 68.0 *b* = 26.3	34.0 (34.0)	(20)	1.0	2.1
			24.6 (24.6)	(11)		
			17.1 (17.2)	(31),(40)		
			13.1 (13.2)	(02)		
			12.1 (12.2)	(22),(51)		
			11.3 (11.3)	(60)		
			4.3 (halo)	–		
KF·**2d**	Col_r at 125 °C *c2mm*	*a* = 67.0 *b* = 25.1	33.5 (33.5)	(20)	1.0	2.3
			23.5 (23.5)	(11)		
			16.7 (16.7)	(31),(40)		
			4.4 (halo)	–		
KF·**2e**	Col_r at 122 °C *c2mm*	*a* = 60.8 *b* = 24.0	30.4 (30.4)	(20)	1.0	2.1
			22.3 (22.3)	(11)		
			15.3 (15.5)	(31),(40)		
			12.0 (12.0)	(02)		
			10.9 (11.2)	(22),(51)		
			10.2 (10.1)	(60)		
			4.9 (halo)	–		
KCl·**2d**	Col_r at 125 °C *c2mm*	*a* = 63.8 *b* = 25.0	31.9 (31.9)	(20)	1.0	2.4
			23.2 (23.2)	(11)		
			16.3 (16.2)	(31),(40)		
			5.0 (halo)	–		
KCl·**2e**	Col_r at 126 °C *c2mm*	*a* = 67.5 *b* = 26.3	33.8 (33.8)	(20)	1.0	2.3
			24.5 (24.5)	(11)		
			16.8 (16.9)	(40),(31)		
			13.3 (13.2)	(02)		
			12.0 (12.0)	(22),(51)		
			11.2 (11.3)	(60)		
			4.6 (halo)	–		
KBr·**2d**	Col_r at 125 °C *c2mm*	*a* = 68.5 *b* = 25.1	34.3 (34.3)	(20)	1.0	2.6
			23.6 (23.6)	(11)		
			17.1 (16.9)	(31),(40)		
			5.1 (halo)	–		
KBr·**2e**	Col_r at 120 °C *c2mm*	*a* = 66.7 *b* = 25.3	33.4 (33.4)	(20)	1.0	2.2
			23.7 (23.7)	(11)		
			16.7 (16.7)	(31),(40)		
			12.7 (12.7)	(02)		
			11.8 (11.9)	(22),(51)		
			4.6 (halo)	–		
KI·**2a**	P at 170 °C	–	–	–	–	–
KI·**2b**	P at 200 °C	–	–	–	–	–
KI·**2c**	Col_r at 170 °C *p2mg*	*a* = 61.6 *b* = 36.0	36.0 (36.0)	(01)	1.2	3.5
			31.1 (31.1)	(11)		
			23.3 (23.4)	(21)		
			17.8 (17.8)	(31)		
			17.4 (17.3)	(12)		
			15.4 (15.4)	(40)		
			14.1 (14.1)	(41)		
			4.3 (halo)	–		
KI·**2e**	Col_r at 150 °C *p2mg*	*a* = 68.7 *b* = 37.9	37.9 (37.9)	(01)	1.2	4.2
			33.2 (33.2)	(11)		
			25.4 (25.5)	(21)		
			19.5 (19.6)	(31)		
			18.3 (18.3)	(12)		
			15.2 (15.6)	(41)		
			12.5 (12.4)	(13)		
			4.8 (halo)	–		

Table 1. (Continued)

Compound	Mesophase	Lattice spacing/ Å	*d* spacing/ Å obsd (calcd)	Miller indices	ρ	$Z^{[a]}$
KBF_4·**2b**	Col_r at 170 °C *p2mg*	*a* = 58.1 *b* = 34.1	34.1 (34.1)	(01)	1.2	3.6
			29.4 (29.4)	(11)		
			22.2 (22.1)	(21)		
			16.9 (16.8)	(31)		
			16.3 (16.3)	(12)		
			4.5 (halo)	–		
KBF_4·**2d**	Col_r at 170 °C *p2mg*	*a* = 62.7 *b* = 36.8	36.8 (36.8)	(01)	1.2	3.6
			31.7 (31.7)	(11)		
			24.1 (23.9)	(21)		
			18.3 (18.2)	(31)		
			17.9 (17.7)	(12)		
			15.9 (15.9)	(22)		
			14.5 (14.4)	(41)		
			12.3 (12.3)	(03)		
			12.0 (12.0)	(13)		
			4.5 (halo)	–		
KBF_4·**2e**	Col_r at 150 °C *p2mg*	*a* = 66.1 *b* = 38.7	38.7 (38.7)	(01)	1.2	3.9
			33.4 (33.4)	(11)		
			25.0 (25.1)	(21)		
			18.9 (19.1)	(31)		
			18.5 (18.6)	(12)		
			16.6 (16.7)	(22)		
			15.2 (15.2)	(41)		
			12.5 (12.7)	(13)		
			4.5 (halo)	–		
KSCN·**2a**	P at 220 °C	–	–	–	–	–
KSCN·**2b**	Col_r at 180 °C *p2mg*	*a* = 58.6 *b* = 34.8	34.8 (34.8)	(01)	1.2	3.5
			29.9 (29.9)	(11)		
			22.6 (22.4)	(21)		
			17.1 (17.0)	(31)		
			16.8 (17.7)	(12)		
			15.0 (15.0)	(22)		
			13.7 (13.5)	(41)		
			11.3 (11.2)	(42)		
			4.2 (halo)	–		
KSCN·**2c**	Col_r at 170 °C *p2gg*	*a* = 48.6 *b* = 46.8	33.7 (33.7)	(11)	1.2	3.9
			23.4 (23.4)	(02)		
			21.0 (20.9)	(12)		
			16.9 (16.9)	(22)		
			13.3 (13.1)	(23)		
			4.5 (halo)	–		
KSCN·**2e**	Col_r at 140 °C *p2gg*	*a* = 53.5 *b* = 47.7	35.6 (35.6)	(11)	1.2	3.8
			26.8 (26.8)	(20)		
			23.6 (23.8)	(02)		
			21.9 (21.8)	(12)		
			17.8 (17.8)	(22)		
			16.7 (16.7)	(31)		
			15.3 (15.2)	(13)		
			14.3 (14.3)	(32)		
			13.7 (13.7)	(23)		
			12.9 (12.9)	(41)		
			11.7 (11.6)	(14)		
			10.2 (10.2)	(43)		
			4.4 (halo)	–		

[a] Calculated by using Equation (1).

nates from overlapping reflections of the alkyl chains in their liquid-like order and the disordered stacking of the aromatic units within the same column.[27,28] For the observed Col_r phases, two planar symmetry groups are possible, namely *c2mm* and *p2gg*.[29] All reflections fulfil the condition for a centered lattice *c*, $h+k=2n$, and hence *c2mm* symmetry can be assigned to the mesophase.[29] Indeed, *p2gg* symmetry would also be possible as the reflections *h*0 and 0*k* satisfy the condition $h=2n$ and $k=2n$,[29,30] but as all reflections fulfil $h+k=2n$, a centered lattice is more likely and is in good agreement with literature data on similar phases.[31] Nevertheless, the assignment should be treated with care because no aligned samples could be obtained. A schematic representation of the Col_r *c2mm* phase of neat **2e** is depicted in Figure 9a.[32] Assuming a density of $\rho = 1.0\,g\,cm^{-3}$, two molecules should be accommodated in the unit cell according to Equation (1).[33]

$$Z = \frac{\rho \cdot N_A \cdot A \cdot h}{M} \quad (1)$$

where Z denotes the number of molecules in the unit cell, ρ = density of the liquid-crystalline phase, N_A = Avogadro's constant, A = columnar cross-section, h = height of a single columnar unit, and M = molecular mass of the liquid crystal. h is obtained from the diffuse scattering in the wide-angle region, which originates from core–core interactions.

The X-ray patterns of complexes KI·**2c**, KI·**2e**, KBF_4·**2b**, KBF_4·**2d**, KBF_4·**2e**, and KSCN·**2b** display a set of reflections at small angles (Table 1, Figure 9b). The presence of (01), (21), and (41) reflections with $h+k=2n+1$ is indicative of a primitive lattice *p*, because these reflections are forbidden in the *c2mm* space group. The (01) reflection violates the condition 0*k*: $k=2n$, thus excluding *p2gg* symmetry; however, the observed reflections are consistent with a *p2mg* plane group (*hk*: no conditions; *h*0: $h=2n$).[34] Thus, a Col_r *p2mg* phase is most likely, in which four molecules are accommodated according to the conditions limiting possible reflections.[29] However, calculation of Z according to Equation (1) yielded $Z \approx 3$. The density, ρ, is likely to be higher than $1.0\,g\,cm^{-3}$. Shibli and co-workers reported a density range of $1.06 \leq \rho \leq 1.08\,g\,cm^{-3}$ for hexaalkyloxytriphenylenes in their mesophase.[35] In the systems KX·**2** with X = I, BF_4, and SCN, the density could even exceed $1.1\,g\,cm^{-3}$ as one equivalent of a potassium salt with a pairing anion (as deduced from NMR spectroscopic results) is dissolved in **2**. Applying $\rho = 1.1–1.2\,g\,cm^{-3}$ in Equation (1) resulted in $Z \approx 4$. A schematic representation of the *p2mg* mesophase geometry is exemplified for KI·**2e** in Figure 9b.

The X-ray diffraction patterns of KSCN·**2c** and KSCN·**2e** are almost identical, but for KSCN·**2e** more reflections are observed, which may be indexed as (11), (20), (02), (12), (22), (31), (13), (32), (23), (41), (14), and (43) (Table 1, Figure 9c). Reflections with $h+k=2n+1$ exclude *c2mm* symmetry for the mesophases of KSCN·**2c** and KSCN·**2e**. The (20) reflection indicates a glide line normal to the crystallographic *y*-axis and the (02) reflection indicates the same symmetry element normal to the *x*-axis. These symmetry elements are only present in the *p2gg* plane group, and therefore *p2gg* symmetry may be assigned to the Col_r phases of KSCN·**2c** and KSCN·**2e**. With a density of $1.1–1.2\,g\,cm^{-3}$, four molecules are accommodated in the cell, which is illustrated

schematically for KSCN·**2e** in Figure 9c. It was surprising that KSCN·**2b** formed a Col_r *p2mg* phase while KSCN·**2c** and KSCN·**2e** displayed mesophases with *p2gg* symmetry. Most probably, the complex with shorter side chains is more comfortably accommodated in a *p2mg* cell.

Conclusion

A series of triphenylene-substituted crown ether derivatives **2a–f** and their potassium complexes KX·**2a–f** have been prepared and investigated, with particular focus on mesomorphic properties and anion effects, both in solution and in the mesophase. Figure 10 presents a comparison of the mesophase temperature ranges of neat and KX-complexed *ortho*-terphenyl-substituted crown ether **1e** and triphenylene-substituted crown ether **2e** bearing undecyl side chains. The extension and flattening of the aromatic system in **2e** and its complexes resulted in increased melting and clearing points. However, with regard to mesophase stabilities, the flatter systems are not always superior to the *o*-terphenyl systems. It is the anion that plays a decisive role in determining the mesophase stabilization. Complexation of crown ether **2e** with potassium salts of hard anions (F^-, Cl^-) or the semi-soft anion Br^- led to mesophases with decreased phase ranges as compared to the corresponding complexes of **1e**. However, the soft anion I^-, which forms tight ion pairs, improved the mesomorphic properties, yielding mesophases with phase ranges of up to 93 °C (KI·**2e**). This effect is even more pronounced in the case of the soft anion SCN^- in KSCN·**2e** ($\Delta T = 132$ °C). In contrast, the corresponding complex KSCN·**1e** formed ordered plastic crystalline phases. The bridging anion BF_4^- induced mesophase stabilization in favor of the triphenylene complex KBF_4·**2e**, whereas PF_6^- led to complete loss of mesomorphism in KPF_6·**2e**. Thus, the bridging abilities of BF_4^- and PF_6^- and their tendencies to induce higher aggregates subtly influence mesophase formation. In the case of the triphenylene complexes, the different counterions (except PF_6^-) induced columnar rectangular mesophases, while the mesophase type of KX·**1** could be changed by appropriate choice of the salt.

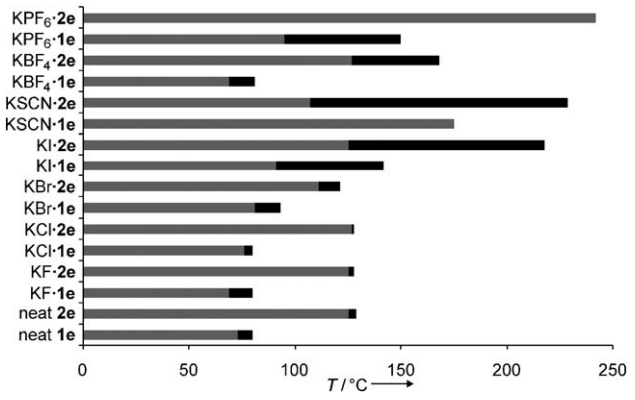

Figure 10. Comparison of the mesophase stabilities of *o*-terphenyl-substituted crown ether **1e** and triphenylene-substituted crown ether **2e** (R = $C_{11}H_{23}$) and their corresponding metal complexes KX·**1e** and KX·**2e**. Key: grey = Cr; black = Col.

The presence of tight ion pairs in the triphenylene complexes KBr·**2**, KI·**2**, and KSCN·**2** with soft anions was indicated by ^1H and ^{13}C NMR spectroscopy, while complexes KBF_4·**2** and KPF_6·**2** with bridging anions were seen to form higher aggregates in solution. These observations are in good agreement with the behavior of the corresponding *o*-terphenyl complexes KX·**1**. However, in comparison to the *o*-terphenyl complexes KX·**1**, the flatter triphenylene complexes KX·**2** show an increased tendency for aggregation in solution, which is most obvious in the spontaneous gel formation of KX·**2**. The amphiphilic structures together with the extended flat aromatic cores seem to strongly favor organogelation, which is in good agreement with observations on phthalocyanine crown ethers.[5b] Furthermore, comparison of the results for KX·**1** and KX·**2** reveals that simply the introduction of strategic C–C bonds in a molecule of molecular weight ~2000 completely changes its supramolecular behavior. This finding may possibly be further extended into a novel design principle for organic gelators.

Experimental Section

General methods: Melting points were measured on a Mettler Toledo DSC822 and are uncorrected. NMR spectra were recorded on Bruker Avance 300 and Avance 500 spectrometers. Unless otherwise stated, spectra were recorded at room temperature. The spectra were calibrated to the respective residual solvent peaks (CD_2Cl_2: $\delta_H = 5.34$ ppm, $\delta_C = 53.40$ ppm; $C_2D_2Cl_4$: $\delta_H = 5.93$ ppm, $\delta_C = 73.99$ ppm). FTIR spectra were recorded on a Bruker Vektor22 spectrometer with an MKII Golden Gate single-reflection Diamant ATR system. MALDI-TOF spectra were recorded on a Bruker Reflex IV spectrometer with a nitrogen laser ($\lambda = 337$ nm); software: XACQ 4.0.4 and XMASS/XTOF 5.1.0. X-ray powder experiments were performed on a Bruker Nanostar; software: SAXS 4.1.26. The samples were kept in Hilgenberg glass capillaries of 0.7 mm outer diameter in a temperature-controlled hot stage (±1 °C). A monochromatic $Cu_{K\alpha 1}$ beam ($\lambda = 1.5405$ Å) was obtained using a ceramic tube generator (1500 W) with cross-coupled Göbel mirrors as the monochromator. The diffraction patterns were recorded on a real-time 2D detector (HI-STAR, Bruker). The patterns were calibrated with the powder pattern of silver behenate. Differential scanning calorimetry (DSC) was performed on the aforementioned Mettler Toledo DSC822, and polarizing optical microscopy (POM) was conducted with an Olympus BX50 polarizing microscope combined with a Linkam LTS350 hot stage and a Linkam TP93 central processor.

Transmission electron microscopy (TEM): Negatively stained samples were prepared at room temperature by spreading 5 μL of a dispersion in $CHCl_3$ onto an Ni grid coated with a Formvar/carbon film. After 10 s, excess liquid was blotted off with filter paper and then 5 μL of 1% aqueous uranyl acetate solution was applied to the grid and drained off after 30 s. The dried specimens were examined with a Zeiss EM 900 transmission electron microscope.

Data for derivatives **2a–d,f** and their complexes KX·**2a–d,f** are summarized in the Supporting Information.

General procedure for the formation of bis[5,6,9,10-tetrakis-(alkyloxy)triphenylene]dibenzo[18]crown-6 ethers: A solution of $FeCl_3$ (0.30 mmol) in nitromethane (1 mL) was added dropwise at 0 °C to a solution of the respective crown ether **1** (0.02 mmol) in absolute CH_2Cl_2

(20 mL), while dry nitrogen was bubbled vigorously through the solution via a cannula. After stirring the mixture for 10 min, the reaction was quenched by the addition of dry methanol (20 mL). The organic layer was washed with H_2O (3×20 mL) and the aqueous layer was extracted with CH_2Cl_2 (3×20 mL). The combined organic layers were dried ($MgSO_4$) and concentrated to yield the pure (elemental analysis) product.

Bis[5,6,9,10-tetrakis(undecyloxy)triphenylene]dibenzo[18]crown-6 ether (2e): Yield: 99%; colorless solid; ^{1}H NMR ($C_2D_2Cl_4$, 355 K, 500 MHz): δ=0.86–0.89 (m, 24H; CH_3), 1.28–1.45 (m, 112H; $O(CH_2)_3(CH_2)_7CH_3$), 1.52–1.59 (m, 16H; $OCH_2CH_2CH_2(CH_2)_7CH_3$), 1.86–1.92 (m, 16H; $OCH_2CH_2(CH_2)_8CH_3$), 4.17 (m_c, 8H; H-b), 4.18 (t, J=6.5 Hz, 8H; $OCH_2(CH_2)_9CH_3$), 4.19 (t, J=6.6 Hz, 8H; $OCH_2(CH_2)_9CH_3$), 4.43 (m_c, 8H; H-a), 7.80, 7.83 ppm (2s, 12H; H_{arom}); ^{13}C NMR ($C_2D_2Cl_4$, 355 K, 125 MHz): δ=14.0 (CH_3), 22.6, 26.2, 29.3, 29.5, 29.6, 29.7, 29.7, 29.7, 31.9 ($OCH_2(CH_2)_9CH_3$), 70.1, 70.4 (OCH_2CH_2O), 70.46, 70.51 ($OCH_2(CH_2)_9CH_3$), 108.4, 108.92, 108.94 (C-3, C-4, C-7, C-8, C-11, C-12), 123.9, 124.1, 124.2 (C-3a, C-3b, C-7a, C-7b, C-11a, C-11b), 149.0, 149.75, 149.79 ppm (C-5, C-6, C-9, C-10); FT-IR (ATR): $\tilde{\nu}$=2918, 2849 (vs), 1618 (m), 1517 (s), 1467 (w), 1436 (vs), 1388 (w), 1260 (vs), 1175 (vs), 1140 (m), 1069 (m), 1045 (m), 835 (m), 721 cm^{-1} (w); MS (MALDI-TOF): m/z: calcd for [$C_{132}H_{212}O_{14}^+$]: 2023.1; found: 2021.8 (100), 1867.2 [$M^+-C_{11}H_{23}$], (47), 1712.5 [$M^+-2C_{11}H_{23}$] (26); elemental analysis calcd (%) for $C_{132}H_{212}O_{14}$ (2023.1): C 78.37, H 10.56; found: C 78.25, H 10.52.

General procedure for the complexation: A solution of **2e** (18.7 μmol) in CH_2Cl_2 (5.0 mL) was added to a solution of the respective potassium salt (28.0 μmol) in MeOH (5.0 mL) and the reaction mixture was stirred overnight at room temperature. After evaporation of the solvent, the residue was taken up in CH_2Cl_2, and the solution was filtered through paper. The filtrate was concentrated in vacuo and the residue was dried under high vacuum to yield the complexes KX·**2e** quantitatively.

Bis[5,6,9,10-tetrakis(undecyloxy)triphenylene]dibenzo[18]crown-6 potassium fluoride complex [KF·2e]: Colorless solid; ^{1}H NMR ($C_2D_2Cl_4$, 355 K, 500 MHz): δ=0.86–0.89 (m, 24H; CH_3), 1.28–1.45 (m, 112H; $O(CH_2)_3(CH_2)_7CH_3$), 1.52–1.59 (m, 16H; $OCH_2CH_2CH_2(CH_2)_7CH_3$), 1.86–1.92 (m, 16H; $OCH_2CH_2(CH_2)_8CH_3$), 4.16–4.21 (m, 24H; H-b and $OCH_2(CH_2)_9CH_3$), 4.43 (m_c, 8H; H-a), 7.80, 7.83 ppm (2s, 12H; H_{arom}); ^{13}C NMR ($C_2D_2Cl_4$, 355 K, 125 MHz): δ=14.0 (CH_3), 22.6, 26.3, 29.3, 29.5, 29.63, 29.66, 29.72, 29.75, 31.9 ($OCH_2(CH_2)_9CH_3$), 70.0, 70.4 (OCH_2CH_2O), 70.4, 70.5 ($OCH_2(CH_2)_9CH_3$), 108.3, 108.9 (C-3, C-4, C-7, C-8, C-11, C-12), 123.9, 124.1, 124.2 (C-3a, C-3b, C-7a, C-7b, C-11a, C-11b), 148.9, 149.74, 149.79 ppm (C-5, C-6, C-9, C-10); FTIR (ATR): $\tilde{\nu}$= 2912, 2852 (vs), 1618 (m), 1518 (s), 1467 (w), 1438 (vs), 1388 (w), 1262 (vs), 1177 cm^{-1} (vs); MS (MALDI-TOF): m/z: calcd for [$C_{132}H_{212}O_{14}K^+$ (M^+-F^-)]: 2062.2; found: 2060.0 (100), 2020.6 [M^+-KF] (45), 1905.2 [$M^+-F^--C_{11}H_{23}$] (15), 1866.0 [$M^+-KF-C_{11}H_{23}$] (17).

Bis[5,6,9,10-tetrakis(undecyloxy)triphenylene]dibenzo[18]crown-6 potassium chloride complex [KCl·2e]: Colorless solid; ^{1}H NMR ($C_2D_2Cl_4$, 355 K, 500 MHz): δ=0.86–0.89 (m, 24H; CH_3), 1.28–1.44 (m, 112H; $O(CH_2)_3(CH_2)_7CH_3$), 1.52–1.59 (m, 16H; $OCH_2CH_2CH_2(CH_2)_7CH_3$), 1.86–1.92 (m, 16H; $OCH_2CH_2(CH_2)_8CH_3$), 4.16–4.21 (m, 24H; H-b and $OCH_2(CH_2)_9CH_3$), 4.43 (m_c, 8H; H-a), 7.80, 7.83 ppm (2s, 12H; H_{arom}); ^{13}C NMR ($C_2D_2Cl_4$, 355 K, 125 MHz): δ=14.0 (CH_3), 22.6, 26.3, 29.3, 29.5, 29.62, 29.66, 29.71, 29.74, 31.9 ($OCH_2(CH_2)_9CH_3$), 70.1, 70.4 (OCH_2CH_2O), 70.4, 70.5 ($OCH_2(CH_2)_9CH_3$), 108.4, 108.9 (C-3, C-4, C-7, C-8, C-11, C-12), 123.9, 124.1, 124.2 (C-3a, C-3b, C-7a, C-7b, C-11a, C-11b), 149.0, 149.73, 149.78 ppm (C-5, C-6, C-9, C-10); FTIR (ATR): $\tilde{\nu}$= 2920 (vs), 2850 (vs), 1618 (w), 1518 (m), 1467 (w), 1438 (s), 1389 (w), 1261 (vs), 1177 (vs), 1137 (w), 1070 (w), 834 (m), 721 cm^{-1} (w); MS (MALDI-TOF): m/z: calcd for [$C_{132}H_{212}O_{14}K^+$ (M^+-Cl^-)]: 2062.2; found: 2060.5 (100), 2020.4 [M^+-KCl] (91), 1905.8 [$M^+-Cl^--C_{11}H_{23}$] (7), 1866.1 [$M^+-KCl-C_{11}H_{23}$] (32).

Bis[5,6,9,10-tetrakis(undecyloxy)triphenylene]dibenzo[18]crown-6 potassium bromide complex [KBr·2e]: Colorless solid; ^{1}H NMR ($C_2D_2Cl_4$, 355 K, 500 MHz): δ=0.86–0.89 (m, 24H; CH_3), 1.28–1.46 (m, 112H; $O(CH_2)_3(CH_2)_7CH_3$), 1.52–1.59 (m, 16H; $OCH_2CH_2CH_2(CH_2)_7CH_3$), 1.86–1.92 (m, 16H; $OCH_2CH_2(CH_2)_8CH_3$), 4.19 (t, J=6.5 Hz, 8H; $OCH_2(CH_2)_9CH_3$), 4.20 (t, J=6.3 Hz, 8H; $OCH_2(CH_2)_9CH_3$), 4.26 (m_c, 8H; H-b), 4.44 (m_c, 8H; H-a), 7.79, 7.80, 7.81 ppm (3s, 12H; H_{arom}); ^{13}C NMR ($C_2D_2Cl_4$, 355 K, 125 MHz): δ=14.0 (CH_3), 22.6, 26.3, 29.3, 29.50, 29.52, 29.63, 29.66, 29.71, 29.76, 31.9 ($OCH_2(CH_2)_9CH_3$), 69.4, 70.0 (OCH_2CH_2O), 70.4, 70.6 ($OCH_2(CH_2)_9CH_3$), 107.4, 108.9, 109.0 (C-3, C-4, C-7, C-8, C-11, C-12), 123.8, 124.1, 124.2 (C-3a, C-3b, C-7a, C-7b, C-11a, C-11b), 148.4, 149.7, 149.9 ppm (C-5, C-6, C-9, C-10); FTIR (ATR): $\tilde{\nu}$=2922 (vs), 2851 (vs), 1618 (w), 1518 (m), 1467 (w), 1439 (s), 1389 (w), 1261 (vs), 1177 (vs), 1137 (w), 1070 (w), 836 cm^{-1} (m); MS (MALDI-TOF): m/z: calcd for [$C_{132}H_{212}O_{14}K^+$ (M^+-Br^-)]: 2062.2; found: 2063.3 (100), 2024.2 [M^+-KBr] (38), 1908.9 [$M^+-Br^--C_{11}H_{23}$] (3), 1869.8 [$M^+-KBr-C_{11}H_{23}$] (9); elemental analysis calcd (%) for $C_{132}H_{212}O_{14}KBr$: C 74.01, H 9.98; found: C 73.72, H 10.08.

Bis[5,6,9,10-tetrakis(undecyloxy)triphenylene]dibenzo[18]crown-6 potassium iodide complex [KI·2e]: Bright-yellow solid; ^{1}H NMR ($C_2D_2Cl_4$, 355 K, 500 MHz): δ=0.86–0.89 (m, 24H; CH_3), 1.28–1.46 (m, 112H; $O(CH_2)_3(CH_2)_7CH_3$), 1.52–1.59 (m, 16H; $OCH_2CH_2CH_2(CH_2)_7CH_3$), 1.86–1.92 (m, 16H; $OCH_2CH_2(CH_2)_8CH_3$), 4.20 (t, J=6.4 Hz, 16H; $OCH_2(CH_2)_9CH_3$), 4.37 (m_c, 8H; H-b), 4.45 (m_c, 8H; H-a), 7.73, 7.77, 7.81 ppm (3s, 12H; H_{arom}); ^{13}C NMR ($C_2D_2Cl_4$, 355 K, 125 MHz): δ=14.0 (CH_3), 22.6, 26.25, 26.27, 29.3, 29.50, 29.54, 29.62, 29.64, 29.67, 29.7, 29.78, 31.9 ($OCH_2(CH_2)_9CH_3$), 68.0, 69.3 (OCH_2CH_2O), 70.4, 70.7 ($OCH_2(CH_2)_9CH_3$), 105.2, 108.8, 109.0 (C-3, C-4, C-7, C-8, C-11, C-12), 123.6, 123.9, 124.3 (C-3a, C-3b, C-7a, C-7b, C-11a, C-11b), 147.0, 149.8, 150.0 ppm (C-5, C-6, C-9, C-10); FTIR (ATR): $\tilde{\nu}$=2920 (s), 2850 (s), 1617 (w), 1517 (m), 1467 (w), 1438 (s), 1389 (w), 1259 (vs), 1177 (vs), 1136 (w), 1069 (w), 835 cm^{-1} (m); MS (MALDI-TOF): m/z: calcd for [$C_{132}H_{212}O_{14}K^+$ (M^+-I^-)]: 2062.2; found: 2059.4 (100), 2020.0 [M^+-KI] (20), 1905.4 [$M^+-I^--C_{11}H_{23}$] (7), 1869.8 [$M^+-KI-C_{11}H_{23}$] (3).

Bis[5,6,9,10-tetrakis(undecyloxy)triphenylene]dibenzo[18]crown-6 potassium thiocyanate complex [KSCN·2e]: Colorless solid; ^{1}H NMR ($C_2D_2Cl_4$, 355 K, 500 MHz): δ=0.86–0.89 (m, 24H; CH_3), 1.28–1.44 (m, 112H; $O(CH_2)_3(CH_2)_7CH_3$), 1.52–1.59 (m, 16H; $OCH_2CH_2CH_2(CH_2)_7CH_3$), 1.86–1.92 (m, 16H; $OCH_2CH_2(CH_2)_8CH_3$), 4.20 (t, J= 6.5 Hz, 16H; $OCH_2(CH_2)_9CH_3$), 4.28 (m_c, 8H; H-b), 4.46 (m_c, 8H; H-a), 7.72, 7.77, 7.81 ppm (3s, 12H; H_{arom}); ^{13}C NMR ($C_2D_2Cl_4$, 355 K, 125 MHz): δ=14.0 (CH_3), 22.6, 26.25, 26.26, 29.3, 29.50, 29.53, 29.58, 29.59, 29.61, 29.62, 29.69, 29.7, 29.8, 31.9 ($OCH_2(CH_2)_9CH_3$), 67.5, 69.2 (OCH_2CH_2O), 70.4, 70.7 ($OCH_2(CH_2)_9CH_3$), 104.6, 108.8, 109.1 (C-3, C-4, C-7, C-8, C-11, C-12), 123.6, 123.8, 124.3 (C-3a, C-3b, C-7a, C-7b, C-11a, C-11b), 146.6, 149.8, 150.0 ppm (C-5, C-6, C-9, C-10); FTIR (ATR): $\tilde{\nu}$=2918 (s), 2849 (s), 2057 (w), 1618 (w), 1517 (m), 1467 (w), 1437 (s), 1390 (w), 1257 (vs), 1176 (vs), 1135 (w), 1068 (m), 1081 (m), 835 cm^{-1} (m); MS (MALDI-TOF): m/z: calcd for [$C_{132}H_{212}O_{14}K^+$ (M^+-SCN^-)]: 2062.2; found: 2062.4 (100), 2022.8 [M^+-KSCN] (32), 1907.6 [$M^+-SCN^--C_{11}H_{23}$] (12), 1869.8 [$M^+-KSCN-C_{11}H_{23}$] (11).

Bis[5,6,9,10-tetrakis(undecyloxy)triphenylene]dibenzo[18]crown-6 potassium tetrafluoroborate complex [KBF$_4$·2e]: Colorless solid; ^{1}H NMR ($C_2D_2Cl_4$, 355 K, 500 MHz): δ=0.87–0.89 (m, 24H; CH_3), 1.29–1.45 (m, 112H; $O(CH_2)_3(CH_2)_7CH_3$), 1.53–1.59 (m, 16H; $OCH_2CH_2CH_2(CH_2)_7CH_3$), 1.86–1.92 (m, 16H; $OCH_2CH_2(CH_2)_8CH_3$), 4.16–4.21 (m, 24H; H-b and $OCH_2(CH_2)_9CH_3$), 4.43 (m_c, 8H; H-a), 7.80, 7.83 ppm (2s, 12H; H_{arom}); ^{13}C NMR ($C_2D_2Cl_4$, 355 K, 125 MHz): δ=14.0 (CH_3), 22.6, 26.25, 29.28, 29.5, 29.62, 29.65, 29.72, 29.74, 31.9 ($OCH_2(CH_2)_9CH_3$), 70.0, 70.3 (OCH_2CH_2O), 70.4, 70.5 ($OCH_2(CH_2)_9CH_3$), 108.3, 108.9 (C-3, C-4, C-7, C-8, C-11, C-12), 123.9, 124.1, 124.2 (C-3a, C-3b, C-7a, C-7b, C-11a, C-11b), 148.8, 149.73, 149.78 ppm (C-5, C-6, C-9, C-10); FTIR (ATR): $\tilde{\nu}$=2918, 2849 (vs), 1617 (m), 1517 (s), 1466 (w), 1437 (vs), 1389 (w), 1262 (vs), 1257 (vs), 1176 (vs), 1136 (m), 1067 (m), 1021 (m), 945 (m), 835 (w), 722 cm^{-1} (w); MS (MALDI-TOF): m/z: calcd for [$C_{132}H_{212}O_{14}K^+$ ($M^+-BF_4^-$)]: 2062.2; found: 2060.7 (100), 2020.8 [M^+-KBF_4] (93), 1905.2 [$M^+-BF_4^--C_{11}H_{23}$] (19), 1866.3 [$M^+-KBF_4-C_{11}H_{23}$] (36); elemental analysis calcd (%) for $C_{132}H_{212}BF_4KO_{14}$: C 73.77, H 9.94; found: C 73.78, H 10.04.

Bis[5,6,9,10-tetrakis(undecyloxy)triphenylene]dibenzo[18]crown-6 potassium hexafluorophosphate complex [KPF$_6$·2e]: Colorless solid; ^{1}H NMR ($C_2D_2Cl_4$, 355 K, 500 MHz): δ=0.87–0.89 (m, 24H; CH_3), 1.28–1.46 (m, 112H; $O(CH_2)_3(CH_2)_7CH_3$), 1.53–1.59 (m, 16H; $OCH_2CH_2CH_2(CH_2)_7CH_3$), 1.87–1.92 (m, 16H; $OCH_2CH_2(CH_2)_8CH_3$), 4.17–4.21 (m,

24H; H-b and $OCH_2(CH_2)_9CH_3$), 4.41 (m_c, 8H; H-a), 7.69, 7.73, 7.79 ppm (3s, 12H; H_{arom}); ^{13}C NMR ($C_2D_2Cl_4$, 355 K, 125 MHz): δ = 14.02, 14.03 (CH_3), 22.6, 26.25, 26.27, 29.29, 29.52, 29.55, 29.64, 29.68, 29.70, 29.78, 31.9 ($OCH_2(CH_2)_9CH_3$), 67.9, 69.0 (OCH_2CH_2O), 70.3, 70.6 ($OCH_2(CH_2)_9CH_3$), 108.7, 108.9 (C-3, C-4, C-7, C-8, C-11, C-12), 123.5, 123.8, 124.2 (C-3a, C-3b, C-7a, C-7b, C-11a, C-11b), 147.0, 149.7, 149.9 ppm (C-5, C-6, C-9, C-10); FTIR (ATR): $\tilde{\nu}$ = 2920, 2850 (vs), 1618 (m), 1518 (s), 1467 (w), 1437 (vs), 1389 (w), 1259 (vs), 1177 (vs), 1137 (m), 1069 (m), 1029 (m), 952 (m), 836 (vs), 722 cm^{-1} (w); MS (MALDI-TOF): *m*/*z*: calcd for $[C_{132}H_{212}O_{14}K^+$ ($M^+-PF_6^-$)]: 2062.2; found: 2061.0 (100), 2021.6 [M^+-KPF_6] (62), 1905.2 [$M^+-PF_6^--C_{11}H_{23}$] (17), 1866.3 [$M^+-KPF_6-C_{11}H_{23}$] (27); elemental analysis calcd (%) for $C_{132}H_{212}F_6KO_{14}P$: C 71.83, H 9.68; found: C 71.72, H 9.73.

Acknowledgements

Generous financial support by the Deutsche Forschungsgemeinschaft, the Max-Planck-Gesellschaft (International Max Planck Research School for Advanced Materials fellowship for M.K.), the Fonds der Chemischen Industrie, the Bundesministerium für Bildung und Forschung, and the Ministerium für Wissenschaft, Forschung und Kunst des Landes Baden-Württemberg is gratefully acknowledged. We would like to thank Prof. Clemens Richert for providing the MALDI-TOF MS equipment as well as the referees and Prof. Frank Giesselmann for their valuable suggestions.

[1] a) S. Sergeyev, W. Pisula, Y. H. Geerts, *Chem. Soc. Rev.* **2007**, *36*, 1902–1929; b) S. Laschat, A. Baro, N. Steinke, F. Giesselmann, C. Hägele, G. Scalia, R. Judele, E. Kapatsina, S. Sauer, A. Schreivogel, M. Tosoni, *Angew. Chem.* **2007**, *119*, 4916–4973; *Angew. Chem. Int. Ed.* **2007**, *46*, 4832–4887; c) T. Kato, N. Mizoshita, K. Kishimoto, *Angew. Chem.* **2006**, *118*, 44–74; *Angew. Chem. Int. Ed.* **2006**, *45*, 38–68; d) S. Kumar, *Chem. Soc. Rev.* **2006**, *35*, 83–109; e) S. Kumar, *Liq. Cryst.* **2005**, *32*, 1089–1113; f) S. Kumar, *Liq. Cryst.* **2004**, *31*, 1037–1059; g) B. Donnio, D. Guillon, R. Deschenaux, D. W. Bruce, *Compr. Coord. Chem. II* **2004**, *7*, 357–627; h) R. J. Bushby, O. R. Lozman, *Curr. Opin. Colloid Interface Sci.* **2002**, *7*, 343–354; i) C. Tschierske, *Annu. Rep. Prog. Chem.* **2001**, *97*, 191–267; j) D. Demus, J. Goodby, G. W. Gray, H.-W. Spiess, V. Vill, *Handbook of Liquid Crystals, Vol. 2B*, Wiley-VCH, Weinheim, **1998**.

[2] a) R. P. Tuffin, G. H. Mehl, K. J. Toyne, J. W. Goodby, *Mol. Cryst. Liq. Cryst.* **1997**, *304*, 223–230; b) R. P. Tuffin, K. J. Toyne, J. W. Goodby, *J. Mater. Chem.* **1996**, *6*, 1271–1282; c) R. P. Tuffin, K. J. Toyne, J. W. Goodby, *J. Mater. Chem.* **1995**, *5*, 2093–2104; d) A. J. Blake, D. W. Bruce, J. P. Danks, I. A. Fallis, D. Guillon, S. A. Ross, H. Richtzenhain, M. Schröder, *J. Mater. Chem.* **2001**, *11*, 1011–1018; e) J. A. Schröter, C. Tschierske, M. Wittenberg, J. H. Wendorff, *Angew. Chem.* **1997**, *109*, 1160–1163; *Angew. Chem. Int. Ed. Engl.* **1997**, *36*, 1119–1121; f) V. Percec, D. Schlueter, G. Ungar, S. Z. D. Cheng, A. Zhang, *Macromolecules* **1998**, *31*, 1745–1762; g) V. Percec, G. Johansson, G. Ungar, J. Zhou, *J. Am. Chem. Soc.* **1996**, *118*, 9855–9866; h) V. Percec, D. Tomazos, J. Heck, H. Blackwell, G. Ungar, *J. Chem. Soc. Perkin Trans. 2* **1994**, 31–44; i) G. Johansson, V. Percec, G. Ungar, D. Abramic, *J. Chem. Soc. Perkin Trans. 1* **1994**, 447–459; j) V. Percec, G. Johansson, J. Heck, G. Ungar, S. V. Batty, *J. Chem. Soc. Perkin Trans. 1* **1993**, 1411–1420; k) V. Percec, G. Johansson, R. Rodenhouse, *Macromolecules* **1992**, *25*, 2563–2565; l) M. Peterca, V. Percec, A. E. Dulcey, S. Nummelin, S. Korey, M. Ilies, P. A. Heiney, *J. Am. Chem. Soc.* **2006**, *128*, 6713–6720; m) C. Tschierske, *J. Mater. Chem.* **1998**, *8*, 1485–1508; n) J. W. Goodby, G. H. Mehl, I. M. Saez, R. P. Tuffin, G. Mackenzie, R. Auzély-Velty, T. Benvegnu, D. Plusquellec, *Chem. Commun.* **1998**, 2057–2070; o) J.-M. Lehn, J. Malthête, A.-M. Levelut, *J. Chem. Soc. Chem. Commun.* **1985**, 1794–1796; p) A. Liebmann, C. Mertesdorf, T. Plesnivy, H. Ringsdorf, J. H. Wendorff, *Angew. Chem.* **1991**, *103*, 1358–1361; *Angew. Chem. Int. Ed. Engl.* **1991**, *30*, 1375–1377; q) J. Malthête, A.-M. Levelut, J.-M. Lehn, *J. Chem. Soc. Chem. Commun.* **1992**, 1434–1436; r) F. Neve, M. Ghedini, O. Francescangeli, *Liq. Cryst.* **1996**, *21*, 625–630.

[3] a) C. F. van Nostrum, *Adv. Mater.* **1996**, *8*, 1027–1030; b) C. F. van Nostrum, R. J. M. Nolte, *Chem. Commun.* **1996**, 2385–2392; c) C. F. van Nostrum, S. J. Picken, A.-J. Schouten, R. J. M. Nolte, *J. Am. Chem. Soc.* **1995**, *117*, 9957–9965; d) C. F. van Nostrum, S. J. Picken, R. J. M. Nolte, *Angew. Chem.* **1994**, *106*, 2298–2300; *Angew. Chem. Int. Ed. Engl.* **1994**, *33*, 2173–2175; e) O. E. Sielcken, M. M. van Tilborg, M. F. M. Roks, R. Hendriks, W. Drenth, R. J. M. Nolte, *J. Am. Chem. Soc.* **1987**, *109*, 4261–4265; f) C. Sirlin, L. Bosio, J. Simon, V. Ahsen, E. Yilmazer, Ö. Bekaroglu, *Chem. Phys. Lett.* **1987**, *139*, 362–364.

[4] a) D. J. Abdallah, R. G. Weiss, *Adv. Mater.* **2000**, *12*, 1237–1247; b) K. Murata, M. Aoki, T. Nishi, A. Ikeda, S. Shinkai, *J. Chem. Soc. Chem. Commun.* **1991**, 1715–1718.

[5] a) M. Gutiérrez-Nava, M. Jaeggy, H. Nierengarten, P. Masson, D. Guillon, A. Van Dorsselaer, J.-F. Nierengarten, *Tetrahedron Lett.* **2003**, *44*, 3039–3042; b) P. Samorí, H. Engelkamp, P. de Witte, A. E. Rowan, R. J. M. Nolte, J. P. Rabe, *Angew. Chem.* **2001**, *113*, 2410–2412; *Angew. Chem. Int. Ed.* **2001**, *40*, 2348–2350; c) H. Engelkamp, S. Middelbeek, R. J. M. Nolte, *Science* **1999**, *284*, 785–788.

[6] a) S. Coco, C. Cordovilla, P. Espinet, J.-L. Gallani, D. Guillon, B. Donnio, *Eur. J. Inorg. Chem.* **2008**, 1210–1218; b) Y. Chen, W. Su, M. Bai, J. Jiang, X. Li, Y. Liu, L. Wang, S. Wang, *J. Am. Chem. Soc.* **2005**, *127*, 15700–15701.

[7] a) U. Beginn, G. Zipp, M. Möller, *Adv. Mater.* **2000**, *12*, 510–513; b) U. Beginn, G. Zipp, A. Mourran, P. Walther, M. Möller, *Adv. Mater.* **2000**, *12*, 513–516; c) U. Beginn, G. Zipp, M. Möller, *Chem. Eur. J.* **2000**, *6*, 2016–2023.

[8] N. Steinke, W. Frey, A. Baro, S. Laschat, C. Drees, M. Nimtz, C. Hägele, F. Giesselmann, *Chem. Eur. J.* **2006**, *12*, 1026–1035.

[9] N. Steinke, M. Jahr, M. Lehmann, A. Baro, W. Frey, S. Tussetschläger, S. Sauer, S. Laschat, *J. Mater. Chem.* **2009**, *19*, 645–654.

[10] See also: a) R. Plehnert, J. A. Schröter, C. Tschierske, *J. Mater. Chem.* **1998**, *8*, 2611–2626; b) G. X. He, F. Wada, K. Kikukawa, S. Shinkai, T. Matsuda, *J. Org. Chem.* **1990**, *55*, 548–554; for [15]crown-5 ether-substituted phthalocyanine mesogens, cation complexation was carried out with Na^+, K^+, Ca^{2+}, and NH_4^+ and the resulting complexes were studied in detail: c) V. Ahsen, E. Yilmazer, M. Ertas, Ö. Bekâroglu, *J. Chem. Soc. Dalton Trans.* **1988**, 401–406; d) N. Kobayashi, A. B. P. Lever, *J. Am. Chem. Soc.* **1987**, *109*, 7433–7441.

[11] I. Bury, B. Heinrich, C. Bourgogne, D. Guillon, B. Donnio, *Chem. Eur. J.* **2006**, *12*, 8396–8413.

[12] M. Kaller, S. Tussetschläger, P. Fischer, C. Deck, A. Baro, F. Giesselmann, S. Laschat, *Chem. Eur. J.* **2009**, *15*, 9530–9542.

[13] P. Herwig, C. W. Kayser, K. Müllen, H. W. Spiess, *Adv. Mater.* **1996**, *8*, 510–513.

[14] Reviews on HBC: a) A. C. Grimsdale, J. Wu, K. Müllen, *Chem. Commun.* **2005**, 2197–2204; b) M. D. Watson, A. Fechtenkötter, K. Müllen, *Chem. Rev.* **2001**, *101*, 1267–1300; c) A. J. Berresheim, M. Müller, K. Müllen, *Chem. Rev.* **1999**, *99*, 1747–1785.

[15] Y. Zhou, W.-J. Liu, W. Zhang, X.-Y. Cao, Q.-F. Zhou, Y. Ma, J. Pei, *J. Org. Chem.* **2006**, *71*, 6822–6828.

[16] For a very recent approach to crown ether-linked triphenylenes, see also: J. Li, Z. He, H. Gopee, A. N. Cammidge, *Org. Lett.* **2010**, *12*, 472–475.

[17] The complexes [NH_4PF_6·**2a**–**f**] were prepared analogously (see the Supporting Information). All of these complexes were found to be non-mesomorphic. Nevertheless, with regard to the anion effect, similar trends were observed in the ^1H and ^{13}C NMR spectra as seen for the corresponding KPF_6 complexes.

[18] C. J. Pedersen, *J. Am. Chem. Soc.* **1967**, *89*, 7017–7036.

[19] C. J. Pedersen, *Org. Synth.* **1972**, *52*, 66–74.

[20] A. Schultz, Dissertation, Universität Braunschweig (Germany), **2003**.

[21] a) H. Maeda, *Chem. Eur. J.* **2008**, *14*, 11274–11282; b) D. J. Abdallah, R. G. Weiss, *Adv. Mater.* **2000**, *12*, 1237–1247; c) J. H. van Esch,

B. L. Feringa, *Angew. Chem.* **2000**, *112*, 2351–2354; *Angew. Chem. Int. Ed.* **2000**, *39*, 2263–2266.
[22] D. Live, S. I. Chan, *J. Am. Chem. Soc.* **1976**, *98*, 3769–3778.
[23] J. C. Lockhart, A. C. Robson, M. E. Thompson, P. D. Tyson, I. H. M. Wallace, *J. Chem. Soc. Dalton Trans.* **1978**, 611–617.
[24] M.-C. Fedarko, *J. Magn. Reson. (1969–1992)* **1973**, *12*, 30–35.
[25] J. D. Dunitz, M. Dobler, P. Seiler, R. P. Phizackerley, *Acta Crystallogr. Sect. B* **1974**, *30*, 2733–2738.
[26] P. Seiler, M. Dobler, J. D. Dunitz, *Acta Crystallogr. Sect. B* **1974**, *30*, 2744–2745.
[27] A. M. Levelut, *J. Chim. Phys.* **1983**, *80*, 149–161.
[28] S. Krishna Prasad, D. S. S. Rao, S. Chandrasekhar, S. Kumar, *Mol. Cryst. Liq. Cryst.* **2003**, *396*, 121–139.
[29] *International Tables for X-ray Crystallography, Vol. I*, Kynoch Press, Birmingham, **1969**.
[30] a) S. Sergeyev, E. Pouzet, O. Debever, J. Levin, J. Gierschner, J. Cornil, R. G. Aspe, Y. H. Geerts, *J. Mater. Chem.* **2007**, *17*, 1777–1784; b) A. Hayer, V. de Halleux, A. Köhler, A. El-Garoughy, E. W. Meijer, J. Barberá, J. Tant, J. Levin, M. Lehmann, J. Gierschner, J. Cornil, Y. H. Geerts, *J. Phys. Chem. B* **2006**, *110*, 7653–7659.
[31] a) V. Percec, J. G. Rudick, M. Peterca, E. Aqad, M. R. Imam, P. A. Heiney, *J. Polym. Sci. Polym. Chem. Ed.* **2007**, *45*, 4974–4987; b) X. Cheng, M. Kumar Das, U. Baumeister, S. Diele, C. Tschierske, *J. Am. Chem. Soc.* **2004**, *126*, 12930–12940; c) F. Morale, R. W. Date, D. Guillon, D. W. Bruce, R. L. Finn, C. Wilson, A. J. Blake, M. Schröder, B. Donnio, *Chem. Eur. J.* **2003**, *9*, 2484–2501; d) B. Heinrich, K. Praefcke, D. Guillon, *J. Mater. Chem.* **1997**, *7*, 1363–1372.
[32] Simple molecular modeling (using ChemBio3D 11.0) was performed. Molecular dimensions of 33 Å × 25 Å were calculated for neat **2e**, indicating that two molecules should be easily accommodated in the unit cell. This finding was supported by the calculation of *Z*.[33]
[33] M. Lehmann, C. Köhn, H. Meier, S. Renker, A. Oehlhof, *J. Mater. Chem.* **2006**, *16*, 441–451.
[34] D. Guillon, in *Structure and Bonding, Vol. 95* (Ed.: D. M. P. Mingos), Springer, Heidelberg, **1999**, pp. 41–82.
[35] V. A. Gunyakov, N. P. Shestakov, S. M. Shibli, *Liq. Cryst.* **2003**, *30*, 871–875.

Received: January 20, 2010
Published online: April 21, 2010

